Electrical and Computer Engineering Faculty
Publications

Department of Electrical and Computer
Engineering

7-1992

Analysis of Multifrequency Dispersive Optical Bistability and Switching in Nonlinear Ring Cavities with Large Medium-Response Times

Pawel Pliszka
Syracuse University

Partha P. Banerjee
University of Dayton, pbanerjee1@udayton.edu

eCommons Citation

Analysis of multifrequency dispersive optical bistability and switching in nonlinear ring cavities with large medium-response times

Pawel Pliszka

Department of Physics, Syracuse University, Syracuse, New York 13244

Partha P. Banerjee

Department of Electrical Engineering, University of Alabama in Huntsville, Huntsville, Alabama 35899

Using a simple model of a ring cavity comprising a cubically nonlinear medium, we analyze dispersive optical bistability in the presence of more than one spectral component. We show the phenomenon of so-called competition for resonance. In addition to presenting cavity characteristics for the cases of two and three different frequencies, we also discuss the general method for finding steady-state solutions and checking their stability. A simple and efficient algorithm, based on a relaxation method, is devised to find steady-state solutions satisfying appropriate boundary conditions. The relaxation dynamics is physically related to a finite response time of the medium.

I. INTRODUCTION

Optical bistability or optical phase transitions, as one should rather call it in general, has been a subject of intensive study over the last two decades. Motivated partly by a hope of possible application to optical computing, several efforts have been made to master the understanding of phenomena of optical bistability, effect of hysteresis, dynamics of switching, and instabilities [1,2]. Although leaving many practical questions still unresolved, these efforts have contributed largely to the physics of nonlinear phenomena, the formulation of problems of optical bistability in the context of the theory of dynamical systems [2,3] and nonequilibrium statistical mechanics [4].

It is our aim in this paper to present some new effects which emerge in a multiwave nonlinear ring cavity (see Fig. 1). Instead of choosing a standard, more challenging, model of resonant interaction of light with a multilevel atomic system [5,6] we investigate these effects using a more phenomenological model of cubic nonlinearity. In essence, our model is similar to that of [7], where a nonlinear ring cavity with two orthogonal polarizations, and with different detunings, is discussed. As mentioned in [7], two optical frequencies interacting incoherently would also obey the same model. In this paper we present steady-state characteristics for such a device, which exhibits interesting phenomena absent in the single-wave models. We would like to point out that two-wave bistability is also discussed under the high-finesse approximation in [8], where some of these phenomena are mentioned. In our work we do not impose this approximation; moreover, our ability to tackle the problem relies neither on the existence of explicit relations between the intensities and the medium variables, nor on the existence of explicit solutions of the propagation equations.

We should stress the difference between our study and those done in the context of Maxwell-Bloch equations in the mean (uniform) field limit. This limit is relevant in the study of many laser systems, but does not hold for an externally driven cavity of low finesse or for a long medium. In such cases propagation of fields must be taken into account.

Our model incorporates the spatial variations of the fields. For the sake of simplicity, we assume that the propagation equations in the steady-state limit can be derived from the nonlinear optics equation.

We discuss the case of coherent and incoherent interactions of two waves, and coherent interaction of three waves (carrier and a sideband pair). Most importantly, we give a very practical numerical tool for finding steady states for an arbitrarily large number of degrees of freedom (e.g., number of different frequency components). Using a concept of relaxation or "slowing down" of the round-trip map, which models the finite response time of the medium, we are able not only to present steady-state input-output characteristics, but also to discuss the stability of its various branches in an almost trivial fashion. It has to be stressed that our model assumes several simplifications. First, the propagation equation is taken to be the cubically nonlinear equation for the optical field only, and the dynamics of the medium is treated phenom-
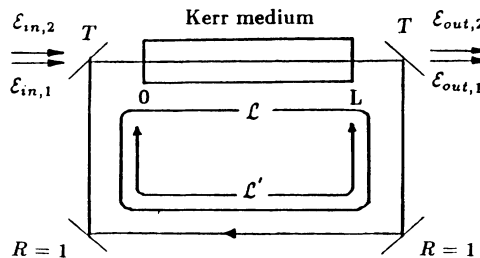

FIG. 1. Nonlinear ring cavity for two incident frequencies.

enologically. Therefore our model does not account for beating between waves [9], as well as for any complicated response of the atomic variables, present, for instance, in a two-level system [5]. Second, the assumption that only specified spectral components propagate inside the resonator is an approximation which may be justified when unwanted frequencies cannot be effectively generated because of, for instance, the phase mismatch between polarization and the electric field. Then the spectral transmission of resonator selects only a given, narrow range of spectral components to experience positive feedback; therefore it seems reasonable to assume that only those optical frequencies which are incident on the cavity are present inside of the cavity. This is in opposition to the study of the propagation of beams or pulses in nonlinear materials where any restriction on the number of spectral components cannot be *a priori* made because of the process of self-phase modulation [10]. We discuss the case of a ring resonator, rather than of a Fabry-Pérot resonator, to avoid complications related to presence of both backward and forward traveling waves, but we believe that the main feature which we refer to as a "competition between waves for resonance" appears for any kind of phasor feedback. Furthermore we do not take into account any transverse degrees of freedom [11,12], thus neglecting possible influence of self-focusing [13] and related effects. Finally, we neglect any effect which may cause saturation of the index of refraction.

Specifically, the layout of the paper is as follows. Section II presents a steady-state analysis. We discuss, in brief, the propagation of two and three waves in the nonlinear material in subsections II B and II C, respectively. The characteristics of the cavity for these two cases are presented in subsections II D and II E. We discuss the case of a symmetrically pumped two-wave cavity, and present important phenomena of selective switching and intensity locking. In Sec. III, using a phenomenological description of the evolution of nonlinearity, we generalize the Ikeda map for the two-wave case and for an active medium with a large response time. We iterate this map numerically to find the steady-state solutions. We should point out that the main emphasis of the paper is on the derivation of the steady-state solutions (cavity characteristics) rather than on the dynamics; this is why we defer discussions of the dynamics to Sec. III. In Sec. IV we discuss the numerical method.

II. STEADY-STATE ANALYSIS

A. Formulation of the problem

To describe the propagation of the scalar optical field $\mathcal{E}$, comprising multiple frequencies, we use a standard ansatz

$$\mathcal{E} = \sum_{j=1}^{N} \mathcal{E}_j(z) e^{i(k_j z - \omega_j t)} + \text{c.c.} \, , \tag{1}$$

where for this section we disregard the temporal dependence of the slowly varying complex envelopes $\mathcal{E}_j$. The equations governing the spatial dependence of $\mathcal{E}_j$ can be formally derived from the nonlinear optics equation [14]

$$\frac{1}{v^2} \frac{\partial^2 \mathcal{E}}{\partial t^2} - \frac{\partial^2 \mathcal{E}}{\partial z^2} = \frac{\beta}{3v^2} \frac{\partial^2 \mathcal{E}^3}{\partial t^2} \, , \tag{2}$$

with β being a cubic nonlinearity coefficient, and where v is the linear phase velocity in the medium. We refer to this equation not as a specific model of interaction of the fields with matter, but rather as a framework providing us with a consistent terminology which can be flexibly applied for different models.

To obtain equations governing the spatial dependence of $\mathcal{E}_j$, we ignore the second-order derivatives of $\mathcal{E}_j$, and make two assumptions. We take $\omega_j = vk_j$ for simplicity. Note that even if $\omega_j \neq vk_j$, the equations which we derive below can be obtained by a simple change of the dependent variable $\mathcal{E}'_j \equiv \mathcal{E}_j e^{iz(\omega_j^2 - v^2 k_j^2)/2k_j v^2}$, provided that terms $\omega_j^2 - vk_j^2$ corresponding to a possible linear dispersion are the same for all waves. Secondly, since we are interested in the case of optical frequencies being very close to each other, i.e., $(\omega_l - \omega_j)/\omega_j < 10^{-5}$, we can replace all k_j's by a single k in the equations describing propagation of different fields, and set $k = 1$ for simplicity. Note that while this assumption is equivalent to neglecting terms of the type $|e^{(ik_l \beta L)} - e^{(ik_j \beta L)}|$, we may not neglect the difference of the linear detunings of each frequency with respect to the resonant frequency of the cavity, related to terms $e^{i\theta_j} \equiv e^{(ik_j \mathcal{L})}$ (where L and $\mathcal{L}$ are the lengths of the active medium and of the resonator, respectively). Linear detunings are different due to the difference of wavelengths, or due to linear birefringence as in the case of two polarizations [7].

Since the fields $\mathcal{E}_j$ exist in a unidirectional ring cavity (see Fig. 1), the amplitude of each field independently obeys a two-point boundary condition, which for the steady state takes the form [1,2]

$$\mathcal{E}_j(0) = \sqrt{T} \, \mathcal{E}_{\text{in},j} + Re^{i\theta_j} \mathcal{E}_j(L) \, , \tag{3}$$

where $\mathcal{E}_{\text{in},j}$ is the input field of each wave, R denotes the reflectivities of the mirrors 1 and 2 (assumed to be the same for all waves), and $T \equiv 1 - R$. The amplitudes $\mathcal{E}_j(L)$ are related to $\mathcal{E}_j(0)$ by the propagation equations discussed below.

B. Propagation of two waves

In the case of two waves, $N = 2$; hence from (1) and (2) we obtain

$$\frac{d\mathcal{E}_1(z)}{dz} = -i\beta \mathcal{E}_1(I_1 + aI_2) \, ,$$

$$\frac{d\mathcal{E}_2(z)}{dz} = -i\beta \mathcal{E}_2(I_2 + aI_1) \, , \tag{4}$$

where $I_j \equiv |\mathcal{E}_j|^2$, and may be readily shown to be constants with respect to z.

The solutions of (4) describe a nonlinearly induced change of the phases of the fields, $\mathcal{E}_j(z) = (I_j)^{1/2} e^{i\phi_j(z)}$, with

$$\phi_1(z) = \beta(I_1 + aI_2)z, \quad \phi_2(z) = \beta(I_2 + aI_1)z \, . \tag{5}$$

The coefficient a is equal to 2 in the case of coherently interacting waves. In the case of incoherent interaction of two waves, or in a diffusion dominated medium [8], as well as in the case of two orthogonal polarizations [7] (within the limits of a scalar analysis of nonlinearity), $a = 1$, so that the index of refraction is proportional to the total incoherent intensity. Note that the nonlinearly induced changes in the index of refraction affecting each wave do not change with z. This is related to the assumption that evolution (generation) of frequencies $2\omega_l - \omega_j$ can be neglected. This restriction is not present in the next section.

C. Propagation of three waves

The propagation of three coherently interacting waves is more interesting because as a result of the interaction the waves exchange energy. Thus the intensities are no longer constant along the active medium but change periodically [15]. We assume $\mathcal{E}$ to be of the form

$$\mathcal{E} = \mathcal{E}_{-1} e^{i(k_{-1}z - \omega_{-1}t)} + \mathcal{E}_0 e^{i(k_0 z - \omega_0 t)}$$
$$+ \mathcal{E}_1 e^{i(k_1 z - \omega_1 t)} + \text{c.c.} , \qquad (6)$$

which describes a propagating carrier and two sidebands, which could originate, for instance, from modulation. Following the lines of Sec. II A, one can show that the propagation of $\mathcal{E}_j$ is given by the following set of equations:

$$\frac{d\mathcal{E}_{-1}(z)}{dz} = -i[\mathcal{E}_{-1}(2I - I_{-1}) + \mathcal{E}_0^2 \mathcal{E}_1^*] ,$$

$$\frac{d\mathcal{E}_0(z)}{dz} = -i[\mathcal{E}_0(2I - I_0) + 2\mathcal{E}_0^* \mathcal{E}_1 \mathcal{E}_{-1}] , \qquad (7)$$

$$\frac{d\mathcal{E}_1(z)}{dz} = -i[\mathcal{E}_1(2I - I_1) + \mathcal{E}_0^2 \mathcal{E}_{-1}^*] ,$$

where $I \equiv I_{-1} + I_0 + I_1$ is the conserved total incoherent power. The last terms on the right-hand side are responsible for the intensity changes which, roughly speaking, are related to scattering from induced dynamical gratings. One can show that the system of Eqs. (7) is completely integrable [15]. Below we present a simplified proof of this fact and restate the results of [15], providing some physical insights.

Motivated by the usefulness of the Hamiltonian approach to the wave interaction [16], we have found that it is possible to introduce a real-valued Hamiltonian $H(\mathcal{E}_{-1}, \mathcal{E}_0, \mathcal{E}_1, \mathcal{E}_{-1}^*, \mathcal{E}_0^*, \mathcal{E}_1^*)$ which allows us to write down "equations of motion" as

$$\frac{d\mathcal{E}_j}{dz} = -i\frac{\partial H}{\partial \mathcal{E}_j^*} , \qquad (8)$$

and the complex conjugate of this equation for evolution of the "conjugate momenta" $\mathcal{E}_j^*$, which are to be treated here as independent degrees of freedom. The Hamiltonian is the sum of two independent constants of motion:

$$H = I^2 + I_0(I_1 - I_{-1})^{1/2}\cos(\Theta) - \frac{I_{-1}^2 + I_0^2 + I_1^2}{4} , \qquad (9)$$

where $\mathcal{E}_j = (I_j)^{1/2} e^{i\phi_j}$, $\Theta(z) \equiv 2\phi_0(z) - \phi_1(z) - \phi_{-1}(z)$. Thus the existence of the Hamiltonian directly gives us one more nontrivial invariant: $H - I^2$. Besides these two constants of motion exists a third, viz., $I_1 - I_{-1}$, corresponding to a "preserved symmetry of the spectrum."

Since the Hamiltonian depends on the phases of the complex fields only through Θ, the knowledge of the three constants of motion makes the set of equations completely integrable, thereby reducing it to effectively a one-dimensional problem. It turns out that the spatial evolution of the intensity of the carrier is the same as a temporal behavior of the position of a ball placed in a quartic gravitational potential

$$V(I_0) = a_4 I_0^4 + a_3 I_0^3 + a_2 I_0^2 + a_1 I_0 + a_0 .$$

The propagation equation for I_0 is therefore of the form

$$\frac{1}{2}\left|\frac{dI_0}{dz}\right|^2 = E - V(I_0) , \qquad (10)$$

where E is reminiscent of the total energy of the mechanical system. Notice that the "potential" and "kinetic" terms are not explicitly separated in the Hamiltonian; therefore V depends on the initial conditions, $I_j(z=0)$, $\Theta(z=0)$, through the coefficients a_i. These coefficients can be expressed in terms of the three above invariants. Of course, for specified values of all the three invariants, there is still freedom for the choice of the initial value of I_0. As is obvious from the form of the invariants, this freedom is, however, restricted, with the restriction being that $I_0(0)$ must lie between two points which turn out to be the first two positive roots of the equation $E - V(I_0) = 0$, since both I_0 and $(dI_0/dz)^2$ are greater than zero, while $a_4 < 0$. This trivally implies that the only possible motion is between these roots, and therefore the most general behavior of I_0 consists of oscillations around the minimum of V which is placed between these roots. Small-amplitude oscillations are of course harmonic, but large-amplitude oscillations may not be symmetric due to the asymmetry of V. Formally, the oscillations of intensities can be written in terms of the elliptic functions [15]; unfortunately formulas expressing period and amplitude of the oscillation by the initial conditions are rather involved. For small intensities of the sidebands the amplitude of the oscillation of the carrier increases linearly with amplitude of each sideband, so the process of energy transfer between the carrier and sideband pair is very efficient. Indeed, the three-wave interaction may be viewed as a simplified model of spectra broadening due to self- and cross-phase modulation [10]. When the intensities of the three waves are comparable, however, the efficiency of the energy exchange is sensitive to the relative phase difference. For instance, for $\Theta(0) = 0$ and $I_{-1}(0) = I_1(0) = \frac{2}{3}I_0(0)$ no energy exchange takes place; the intensities remain constant with z [15].

D. Two-wave resonator characteristics

Below we discuss how the solutions of (4) obeying the boundary condition (3) depend on the parameters $E_{in,j}$, which can be taken to be real. The numerical method for

finding the steady-state solution and checking its stability are described in the next two sections, together with the discussion of the dynamics, for purposes of comparison. Now, for the sake of simplicity, since we have two independent variables $I_{in,j} \equiv |\mathscr{E}_{in,j}|^2$, $j = 1, 2$, and two dependent variables $I_{out,j} \equiv |\mathscr{E}_{out,j}|^2$, we restrict ourselves to the case when the two input intensities change proportionally and remain comparable. Practically such a situation could be realized by splitting light from a single quasimonochromatic source, by passing it through two Fabry-Pérot resonators of slightly different lengths, and then by superimposing the beams at the input of the nonlinear ring resonator. The general case of asymmetric pumping is more complicated to describe, because the state of the device depends on the particular path one follows in the input plane $(I_{in,1}, I_{in,2})$.

In what follows, we focus our attention on the dependence of the characteristics on the difference between the linear detunings $\Delta\theta \equiv \theta_2 - \theta_1$.

Because each wave experiences a different linear detuning, one may expect that the two frequencies will never be at resonance together. For the incoherent case ($a = 1$) it is obvious, since the nonlinear phase shifts ϕ_1, ϕ_2 will always be the same for both waves. The behavior of the system depends on the position of the two linear detunings on the linear transmittivity-versus-detuning curve (see insets in Figs. 2 and 3). The effect of nonlinearity manifests itself in an intensity-dependent shift of this curve. For $\beta > 0$, the curve is shifted to the left for increasing intensities.

In the case of $a \neq 1$ and $\Delta\theta = 0$, which may be the case where two orthogonal polarizations interact via nonlinearity of a tensorial nature (e.g., via light-induced quadrupole moment), and the birefringence is absent, we observe nondeterministic symmetry breaking, as reported in [8,17,18]. This means that when the cavity is symmetrically pumped, i.e., $I_{in,1} = I_{in,2}$, and the linear detunings are the same, the output intensities are not equal, and it is impossible to predict which is greater. This happens for sufficiently large intracavity intensities, when the symmetric steady-state solution becomes unstable, and two asymmetric stable solutions emerge [see Fig. 3(a)]. The process can be intuitively understood as a second-order, symmetry-breaking, phase transition. In a more realistic model which takes into account fluctuations of phases, one should expect possible switching between these two asymmetric solutions, as we see in our numerical simulations. It implies that the output intensity of each wave may nondeterministically jump, such that the total output intensity stays constant.

Figures 2 and 3 show the behavior of the output intensity of each wave as a function of the input intensity, both for the cases of coherent and incoherent interaction. These graphs should be regarded as a projection of a curve (in general self-intersections are possible) imbedded in three dimensions $(I_{in}, I_{out,1}, I_{out,2})$ on the planes $(I_{in}, I_{out,1})$, $(I_{in}, I_{out,2})$. (In the figures we show only the branches of characteristics corresponding to the increase of the input intensities.) Observe that in the case where $\Delta\theta$ is greater than the width of the transmission curve

$\sim T$ but smaller than π, the wave with the smaller linear detuning $\mathscr{E}_2$ is never in resonance with the cavity. It explains the lack of "up-switching" of $I_{out,2}$.

The discontinuous change (first-order phase transition), familiar from the single-wave optical bistability is, in the case of the higher frequency, replaced by a discontinuity of the derivative $dI_{out,2}/dI_{in}$ [see Fig. 2(c)]. In spite of the lack of up-switching of $\mathscr{E}_2$, the two-wave system exhibits typical features of first-order phase transitions; transition is accompanied by a change of energy inside the resonator and through the effect of hysteresis. For the decreasing input intensity a small "down-switching" for $\mathscr{E}_2$ occurs.

In passing, we remark that in order to rigorously interpret optical bistability in the language of statistical mechanics, one needs to incorporate fluctuations into the description. (In principle, by solving a resulting Fokker-Planck equation for the probability distribution of the complex fields, one could derive thermodynamic potentials and other thermodynamical variables of interest [2,4].) Therefore we refer here to the language of thermodynamics only at the phenomenological level [2], invoking the analogy with a first-order, liquid-gas, phase transition. Here, the inverse of the strength of coupling (roughly R^{-1}), rather than the strength of the fluctuations, can be compared to the temperature of the liquid-gas system and I_{in} can be viewed as the applied pressure. Whereas in the case of the single wave the intracavity intensity plays the role of the scalar order parameter (e.g., average density), here, in order to distinguish between different fields, one should rather invoke an analogy with multicomponent systems.

In our discussion we will not invoke the temperature parameter since we are interested rather in strong couplings $R > 0.1$, $\beta I_{in} kL \sim 1$. This corresponds to a system being well below "the critical temperature" for the transition. In other words we do not pay much attention to the onset of the switching in relation to the parameters of the cavity. We show different plots to stress the dependence of characteristics on the position of the linear detunings (see Fig. 2).

Next, to explain qualitatively the behavior of the two frequencies in the cavity, we use a phenomenological argument based on the left shift of the transmission curve ($\beta > 0$) or equivalently right shift of detunings. When the cavity is gradually tuned to $\mathscr{E}_2$ by the increase of the intracavity intensity, $\mathscr{E}_1$ is also tuned toward resonance (see Fig. 2 or 3). The state in which $\mathscr{E}_2$ will be exactly in resonance is typically unstable because any spontaneous increase of the intracavity intensity will tend to grow. $\mathscr{E}_1$ will experience a tuning effect; so with the increase of I_{in}, it will grow much faster than $\mathscr{E}_2$ can decrease. This is because at the point of resonance, the transmittivity for $\mathscr{E}_2$ is at the maximum and it is not sensitive to small changes of the intracavity intensities, unlike the transmittivity for $\mathscr{E}_1$. Resonance for $\mathscr{E}_1$ can in turn be stable, for the same reason as in the single-wave case. Observe that for $\Delta\theta > \pi$, when the differential gains or, equivalently, slopes of the transmission curve at θ_1 and θ_2, are comparable, the above arguments do not apply and the behavior is

more complicated [see Figs. 3(c) and 3(d)]. In such cases one can also see down-switching of $I_{out,2}$ even for symmetric pumping. Down-switching has indeed been observed experimentally in a semiconductor device [19] for the case of asymmetric pumping (i.e., where $I_{in,1}$ plays

the role of the independent parameter, while $I_{out,2}$ is the dependent variable). In terms of effective one-dimensional characteristics (i.e., one independent parameter and one dependent variable), it corresponds to a reverse hysteresis curve.
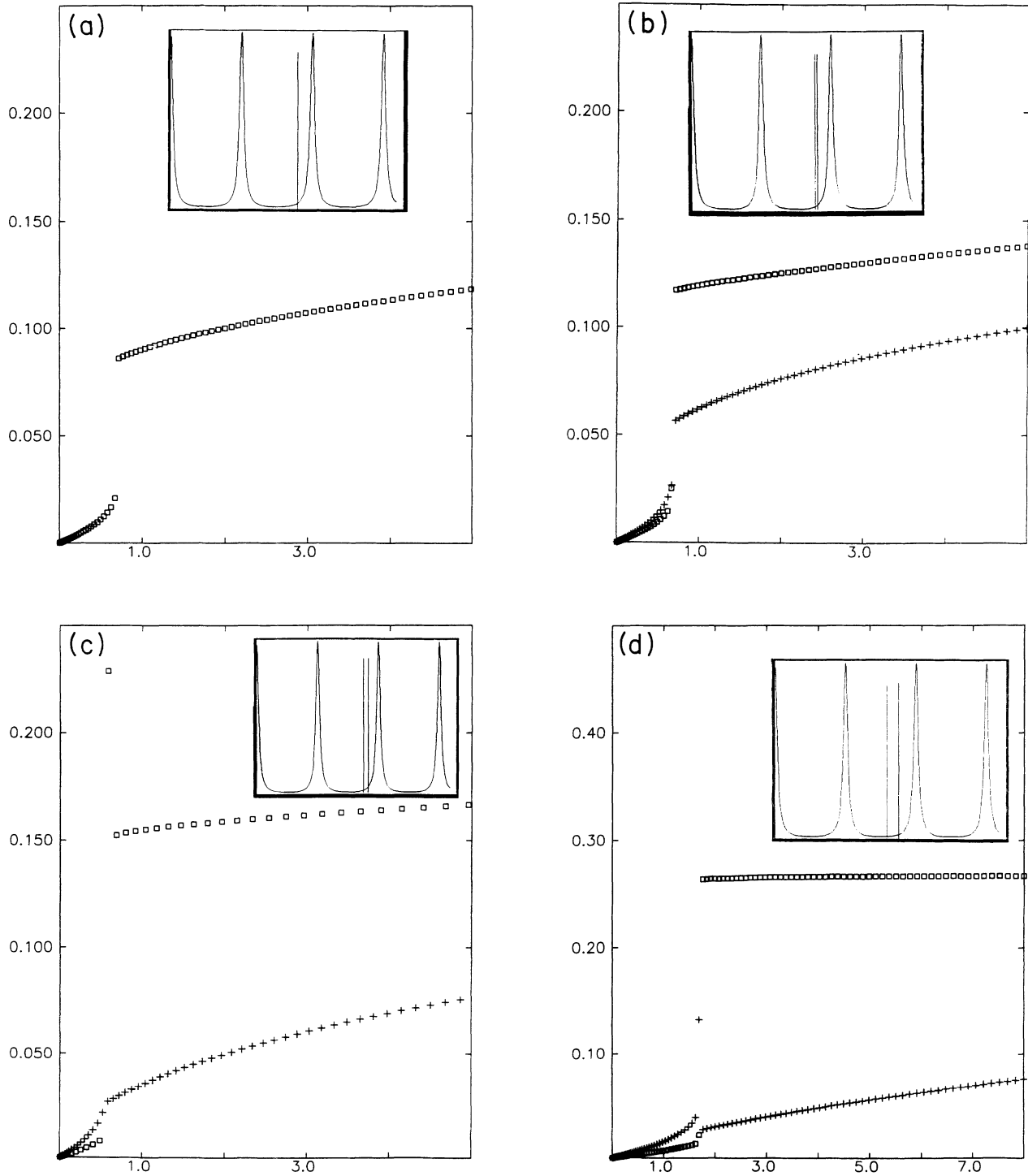

FIG. 2. Output intensities of the incoherently interacting waves vs the input (increasing) intensity for symmetric pumping $(I_{in} = I_{in,1} + I_{in,2}, I_{in,1} = I_{in,2}, \beta k L = 1, R = 0.8)$. Separate plots (a)–(d) correspond to different linear detunings. Insets show the linear transmittivity-vs-detuning curve and the positions of the two linear detunings θ_1, θ_2 (left vertical line corresponds to θ_1). In (b)–(d), crosses represent $I_{out,2}$, squares $I_{out,1}$. Each point of the characteristics was obtained after 200 iterations of the map (18).

By changing $\Delta\theta$, we alter between self-tuning (as in single-wave limit) and cross-detuning effects (competition for resonance). These features are similar for both coherently and incoherently interacting waves. What is different between the two cases is the exact shape of the characteristics. For the case of coherent interaction, due

to larger cross tuning than the self-tuning (i.e., $\partial\phi_1/\partial I_2 > \partial\phi_1/\partial I_1$), the output intensity $I_{\text{out},1}$ will not be a monotonic function of the input intensity. Past the switching point an increase of the input intensity causes a linear increase in the I_2. This is because for $\Delta\theta > T$, $\mathcal{E}_2$ is far from resonance and on the flat part of the transmis-
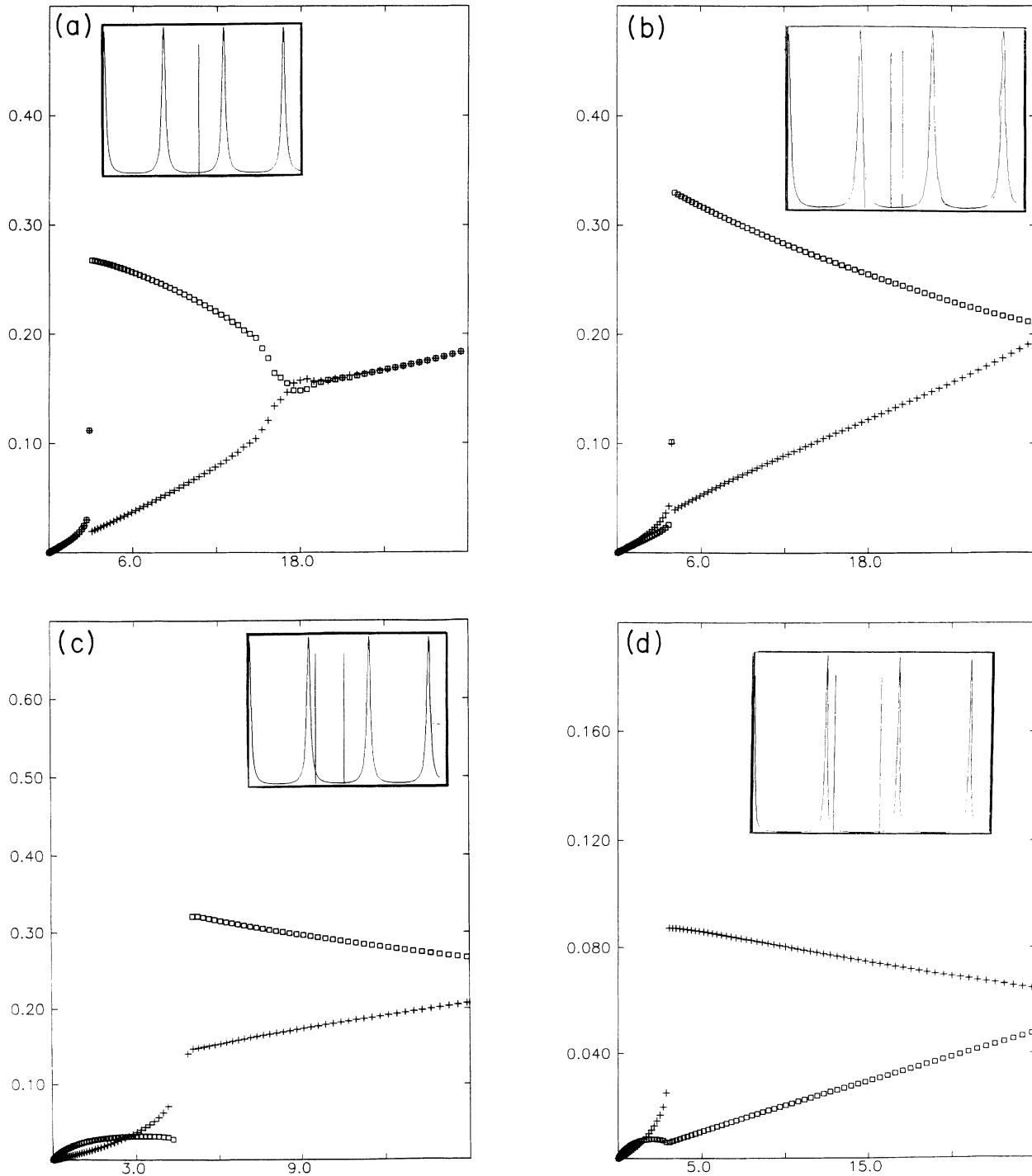

FIG. 3. The same as Fig. 2 for the case of coherently interacting waves, i.e., $a = 2$. For $\Delta\theta = 0$, see plot (a), one can see the symmetry-breaking solution. Dots represent total incoherent output intensity $I_{\text{out},1} + I_{\text{out},2}$ which under appropriate conditions is locked after the switching; see plots (b) and (c).

sion curve, and the cavity behaves as a linear device for $E_{in,2}$. This in turn causes destructive linear detuning for $\mathscr{E}_1$, resulting in a decrease of $I_{out,1}$. Since these two linear effects are of opposite nature, the sum of output intensities remains constant with the increase of the input intensities (signifying locking). This phenomenon of an exact locking of output occurs when $I_{in,1} = I_{in,2}$ but this condition is not very critical (a difference of 10% does not affect the characteristics). For the case of incoherent interaction (and symmetric pumping), the total intensity input-output relation is a monotonic, while the value of $I_{out,1}$ is approximately locked after the first switch up.

The locking of the output may prove useful for possible applications as a power stabilizer or "digitizer" for optical computing. This phenomenon has been mentioned in the early works [20], but rather as an approximate effect.

E. Three-wave resonator characteristics

It is now our task to examine how the energy exchange process can affect the input-output characteristics of the nonlinear ring resonator. We again assume that the intensities of the three waves change proportionally at the input. One can see from Fig. 4(a) that the symmetry of the spectrum of the input field is broken at the output. This, as in the two-wave case, is simply a result of the difference in the linear detunings. Besides phenomena familiar from the two-wave case, it should be noted that the structure of the input-output characteristics becomes much more rich. Even if the cavity is originally detuned and the intensities of the input increase proportionally, one may see large down-switching of the output intensities of the separate waves and nonmonotonicity of the total output incoherent (i.e., time-dependent) intensity I_{out}, see Fig. 4(b). The effect of the change of the index of refraction is twofold; as in the previous cases it tunes the cavity towards resonances, and also changes the value of $\Theta(0)$, which in turn affects the energy transfer efficiency. Since at a first glance these two effects are not simply related, the input-output diagrams become much more complex, and depend on the relative phase of fields injected into the nonlinear medium. The regions of the input intensity corresponding to a dominance of a specific frequency become much narrower; so do the regions of the hysteresis effects.

It should be noted that although the case of incoherent interaction of three, or more, waves is certainly more complicated than the discussed case of two waves, we expect that all the resulting phenomena can be understood in similar terms since the relative phases of the injected fields do not play any role in the incoherent interaction.

We remark that when the intensities of the sidebands are much smaller than the carrier intensity there are no new dramatic effects as compared to the single-wave case, since only the carrier frequency comes into resonance with the cavity.

Finally, before presenting the method used to find the steady-state solutions, we stress that in the multiwave case, in spite of the independence of the boundary condition (3) for each wave, one cannot apply the one-dimensional technique for each wave separately [involv-

ing assuming some N-independent quantities $\mathscr{E}_j(0)$, $j = 1, \ldots, N$ and then solving for $\mathscr{E}_{in,j}$]. Although such a method will yield a solution formally, it will be generally unstable. Moreover, the curve in the input space, $I_{in,j}$, obtained this way can be physically meaningless. From
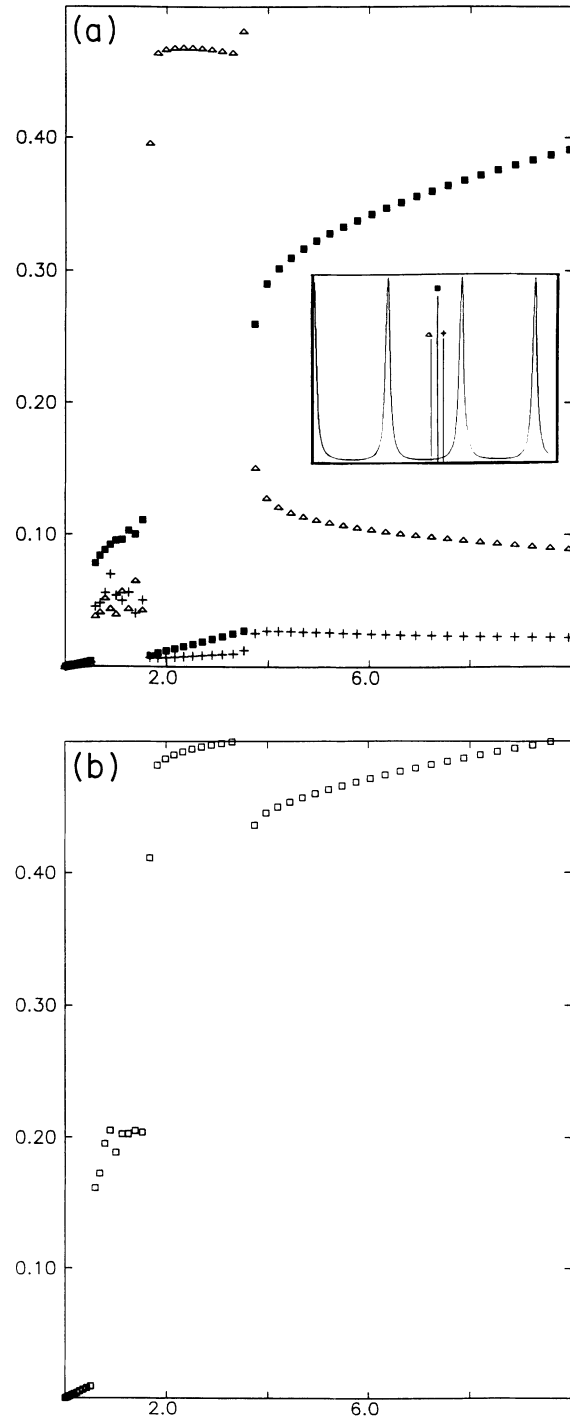

FIG. 4. (a) Input-output characteristics for the three coherently interacting waves, in the case of symmetric pumping and different phases of the pumping fields (shown for the increasing input intensities). Squares represent $I_{out,0}$; crosses, $I_{out,1}$; triangles, $I_{out,-1}$. (b) Input-output characteristics for the sum of intensities.

the above results, it should be obvious that the different fields inside the resonator cannot be set independently, and implying any relations between them on the basis of the knowledge of the incident fields is insurmountably difficult.

III. DISCUSSION OF THE STABILITY AND DYNAMICS

In order to discuss the stability of the steady states, one needs to incorporate dynamics of the medium to the model. We limit ourselves to the phenomenological description, in which medium variables are represented by a single scalar variable—the nonlinear susceptibility [21]. We also restrict the description to the case of two waves. The coupled equations for the electric field and susceptibility are

$$\frac{1}{v^2}\frac{\partial^2 \mathscr{E}}{\partial t^2} - \frac{\partial^2 \mathscr{E}}{\partial z^2} = \frac{\omega^2}{v^2}\chi(z,t)\mathscr{E} , \tag{11a}$$

$$\tau_m \frac{\partial \chi}{\partial t} = -\chi + \frac{\beta}{2}\langle \mathscr{E}^2 \rangle , \tag{11b}$$

where $\langle \ \rangle$ denotes average over rapid oscillations, and τ_m is the medium response time. In the slowly varying envelope approximation, and for the case of incoherent interaction of two waves we get the following set of equations in terms of the variables $(\zeta,\tau)\equiv(z,t-z/v)$:

$$\frac{\partial \mathscr{E}_j}{\partial \zeta} = -i\mathscr{E}_j\chi , \tag{12a}$$

$$\tau_m \frac{\partial \chi}{\partial \tau} = -\chi + \beta(|\mathscr{E}_1|^2 + |\mathscr{E}_2|^2) . \tag{12b}$$

The time-dependent boundary conditions are

$$\mathscr{E}_j(0,\tau) = \sqrt{T}\,\mathscr{E}_{\text{in},j} + \text{Re}^{i\theta_j}\mathscr{E}_j(L,\tau-\tau_r) , \tag{13}$$

where $\tau_r \equiv (\mathcal{L}-L)/c + L/v$ is the round-trip time.

Following the procedure described in [22], we will show that the problem can be reduced to a system of difference-differential equations. We can formally integrate (12a) to get

$$\mathscr{E}_j(\zeta,\tau) = \mathscr{E}_j(0,\tau)e^{-i\eta(\zeta,\tau)} . \tag{14a}$$

Also, from (12b),

$$\tau_m \frac{\partial \eta(\zeta,\tau)}{\partial \tau} = -\eta + \beta I(0,\tau)\zeta . \tag{14b}$$

In the above equation $I = |\mathscr{E}_1|^2 + |\mathscr{E}_2|^2$, and $\eta(\zeta,\tau) \equiv \int_0^\zeta \chi(z,t)dz$ and represents the nonlinear phase shift of the fields (we have assumed χ to be real). The above equations may be used to relate $\mathscr{E}_j(L,\tau-\tau_r)$ with $\mathscr{E}_j(0,\tau)$. This combined with the boundary condition (3) gives the relation between fields at $z=0$ at subsequent instances of time, separated by the round-trip time.

$$\mathscr{E}_j(0,\tau) = \sqrt{T}\,\mathscr{E}_{\text{in},j}(\tau) + \text{Re}^{i[\theta_j - \eta(\tau-\tau_r)]}\mathscr{E}_j(0,\tau-\tau_r) , \tag{15}$$

where the total nonlinear phase shift $\eta(t)$ is defined as

$$\eta(\tau) = \eta(L,\tau) , \tag{16}$$

and obeys an evolution equation

$$\tau_m \frac{d\eta(\tau)}{d\tau} = -\eta + L\beta I(0,\tau) . \tag{17}$$

Now, assuming that the fields do not change substantially during the time τ_r ($\tau_m \gg \tau_r$), we can approximately integrate the last equation over a period τ_r, and reduce the system to a discrete-time mapping:

$$\eta_{n+1} = \eta_n(1-\alpha) + \alpha L\beta I_n , \tag{18a}$$

$$\mathscr{E}_{1,n+1} = \sqrt{T}\,\mathscr{E}_{\text{in},1} + \text{Re}^{i(\theta_1 - \eta_n)}\mathscr{E}_{1,n} , \tag{18b}$$

$$\mathscr{E}_{2,n+1} = \sqrt{T}\,\mathscr{E}_{\text{in},2} + \text{Re}^{i(\theta_2 - \eta_n)}\mathscr{E}_{2,n} , \tag{18c}$$

where $\alpha \equiv 1 - e^{-\tau_r/\tau_m}$.

This map is a multidimensional extension of the Ikeda map to the case of two complex fields, coupled to each other through the total nonlinear phase shift η, which is no longer adiabatically eliminated. Equation (18) may be simply generalized to allow different phase shifts for each wave, and a nonlinear absorption through a complex η. (Linear absorption may be, of course, incorporated in the values of R.)

The form of the map (18a) naturally suggests the concept of what we call "relaxed maps." Let us discuss this concept as simply as possible, assuming for a moment a "uniform relaxation" of all variables. Given a map $x_{n+1} = \mathscr{F}(x_n)$ (x can be a scalar or a vector), we define its α (uniform) relaxation $\mathscr{F}_\alpha$ ($0 < \alpha < 1$) as a map given by

$$x_{n+1} = \mathscr{F}_\alpha(x_n) \equiv \alpha\mathscr{F}(x_n) + (1-\alpha)x_n . \tag{19}$$

It is trivial to check that the fixed points of both maps are the same. However, their stability is usually different. The eigenvalues of the linearized problem (i.e., eigenvalues of the Jacobian matrix at the fixed point) for the relaxed map are given by the simple relation

$$\tilde{\lambda}_\alpha = 1 + \alpha(\lambda - 1) . \tag{20}$$

Equation (20) states that the eigenvalues $\tilde{\lambda}_\alpha$ of the "relaxed" problem are obtained by multiplying the (complex) eigenvalue λ of the original problem by α and by shifting the result to the right by $1-\alpha$. After this operation all eigenvalues lie in the complex plane in the vicinity of 1, i.e., inside a circle centered at $1-\alpha$ with radius proportional to α. Since the criterion for stability is $|\lambda| < 1$, by taking α to be sufficiently small, the oscillatory instabilities related to $\text{Re}(\lambda) < 0$, and also others (see Fig. 5) can be removed, while the "blow-up" instabilities related to $\text{Re}(\lambda) > 1$ are preserved in the relaxation.

The difference between uniform relaxation of all variables (corresponding to α being a scalar), and relaxation of only medium variables (corresponding to α being a diagonal matrix) is in our case of secondary importance for the stability of the steady state. (The steady-state solution is, of course, again independent of α.) Notice that in the limit of $\alpha \to 0$, the reduced maps for fields are linear and have eigenvalues satisfying $|\lambda_i| = R < 1$. Therefore the stability of fixed points can always be enforced by the
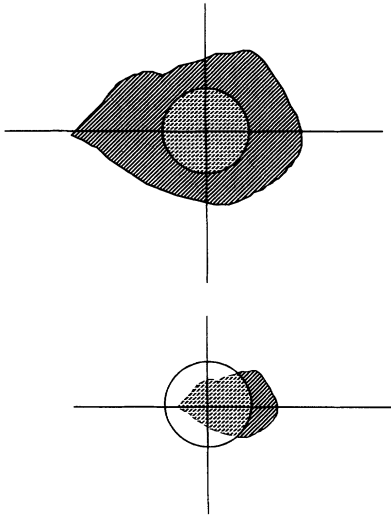
FIG. 5. Diagram illustrating the effect of the relaxation on the complex space of eigenvalues of the Jacobi matrix; see Eq. (20).

sufficiently slow medium response. Although for the case of nonuniform relaxation Eq. (19) is no longer valid, and the corresponding relation between eigenvalues in general cannot be simply stated, one can check that as far as the stability of the steady state is concerned, the only difference between this case and the former is in the actual values of α necessary to provide the stability.

In the simplest case, when the index of refraction de-

pends only on the sum of intensities, Ref. [7] gives analytical criteria for stability, stating that the sum of the inverse of differential gains should not exceed unity. [This criterion checks only against the "blow-up" instability related to $\mathrm{Re}(\lambda) > 1$.] However, in order to apply such criteria, one would need to know the steady-state solution, while our method directly relates the stability condition with parameters which are explicitly present in the problem.

As an illustration we show, in Fig. 6, the stability diagram for the case of two incoherently interacting waves in the (I_{in}, α) plane.

On this diagram one can see a characteristic region of oscillatory instability of the upper branch surrounding the point of the transition for I_1 (for the increasing input intensity). This type of instability is related to the competition for resonance and is different from the one observed in the single-wave optical bistability.

Numerical simulations show stability of the first two branches of characteristics for the two-wave case provided that medium-response time τ_m is a few times larger than round-trip time τ_r. In the multiwave case for $\Delta\theta \gg T$ we do not see any dramatic changes in stability, i.e., in the maximal values of α allowing stability of the steady state, as compared to the single-wave case. However, both the stability diagrams and the form of instabilities for the two-wave and one-wave cases are different. For $\Delta\theta \sim T$, we see oscillatory instability far in the upper branch even for relatively slow media $(\tau_r/\tau_m \sim 0.05)$. This implies that dynamical competition for resonance is particularly pronounced when the separation between the
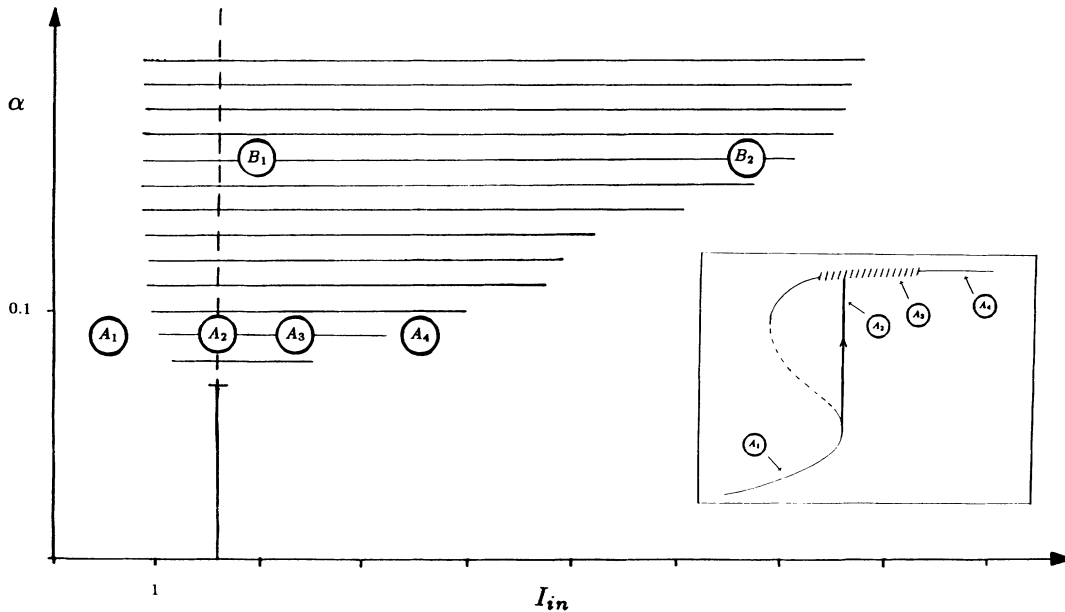

FIG. 6. Approximate stability diagram for the map (18) (steady-state characteristics drawn in inset) in terms of the variables I_{in} (symmetric pumping) and α. Shaded region corresponds to oscillatory instability. Vertical line corresponds to the resonance (switch up) for increasing input intensity. The diagram depends strongly on $\Delta\theta$ due to the "competition for resonance" [here $\theta_1 = 10$, $\theta_2 = 11$, rest of parameters as in Fig. 2(d), which corresponds to $\alpha = 0.05$]. The time dependence of the total intensity for the marked points in parameter space is shown in Fig. 7. Inside of the region of instability shown, only periodic and quasiperiodic evolution are possible. There exist other regions of instabilities corresponding to larger I_{in}, not shown in the figure, which yield both quasiperiodic and chaotic oscillations of intensities; see Fig. 7, plot C_2.

frequencies is of the order of the spectral range of the resonator.

The steady state, when it is stable, is approached in the quasicontinuous evolution either monotonically (see Fig. 7, plot A_1) (for the lower branch of the characteristics) or in decaying oscillations (see Fig. 7, plot A_4) (for the upper part of the characteristics). Oscillatory approach of the steady state is related to the appearance of two complex-conjugate eigenvalues λ. This is a general feature present for two waves as well as for a single wave, which is also familiar in the context of Maxwell-Bloch equations [23]. As is evident from the possible oscillatory approach of the steady state (even in the single-wave case), the quasicontinuous dynamics cannot be effectively explained in the terms of the intensities only, and one should expect that for N fields the problem has intrinsically at least $2N + 1$ (real) degrees of freedom.

When the steady state becomes unstable, the dynamics takes a form of quasiperiodic oscillations (see plots B_1, B_2 in Fig. 7).

For much higher input intensities chaotic oscillations of output intensities are possible even for relatively slow media ($\alpha < 0.1$), as shown in plot C_2 in Fig. 7.

In the stable regime, far from bifurcation points, the short time scale τ_r, related to the discrete-time character of the evolution, does not manifest itself in the dynamics of the fields, and besides few initial oscillations one sees quasicontinuous evolution of the intensities. However,

FIG. 7. The I_{out} vs time dependence shown for times up to $300\tau_r$. Plots A and B correspond to different values of α and I_{in} as shown in Fig. 6. Plot C_1: $a = 2$, $\alpha = 0.03$, $I_{\text{in}} = 15$, $\Delta\theta = 0$. Plot C_2: $a = 1$, $\alpha = 0.05$, $I_{\text{in}} = 15$, $\Delta\theta \sim T$.

when the fixed point becomes unstable fields may change significantly during τ_r and the reduction of the differential equation (17) to a map may no longer be legitimate. Equation (17) integrated over one round-trip time gives

$$\eta(\tau_r) = \eta(0)e^{-\tau_r/\tau_m} + \frac{\beta}{\tau_m}\int_0^{\tau_r} I(0,\tau)\exp\left[\frac{\tau - \tau_r}{\tau_m}\right] d\tau ,$$

(21)

and involves the unknown function $I(0,\tau)$. Note that for this reason the local stability of a fixed point does not strictly imply the stability of the steady-state solution of the corresponding partial differential equation. However, the stability of the fixed point combined with structural stability of the map [stability against perturbations of the functional dependence of η_n on I_{n-1} reflecting the relation between I_{n-1} and time average of $I(\tau)$ present in (21)], would imply the stability of the system. We did not perform the structural stability of the map.

IV. NUMERICAL METHOD

The relaxed map approach, regardless of its limitation for the description of the dynamics, is useful as a numerical tool for finding the steady-state cavity characteristics [24]. In general, the form of the map should be chosen in such a way that the fixed-point fields will satisfy the steady-state boundary conditions (3). The choice of such a map is, of course, not unique and should be motivated by the dynamics of the medium. For the purpose of numerical simulation alone, the simplest choice is the uniformly relaxed map. For example, in the case of three waves the presented steady-state solution is a fixed point of the round-trip map

$$\mathcal{E}_j(0,(n+1)\tau_r) = \alpha[\sqrt{T}E_{\text{in},j} + \text{Re}^{i\theta_j}\mathcal{E}_j(L,n\tau_r)]$$

$$+ (1-\alpha)\mathcal{E}_j(0,n\tau_r) , \qquad (22)$$

with the terms $\mathcal{E}_j(L,n\tau_r)$ obtained by integration of the steady-state propagation equations (7) with the initial condition given by $\mathcal{E}_j(0,n\tau_r)$. For sufficiently small α, iterations always converge to one of the fixed points. This map may, of course, not model the physical dynamics [25], but nevertheless is useful as a tool for finding the steady-state solutions, which can be applied to an arbitrary number of frequencies. Given some additional specific information about the medium, allowing separation of the fast and the slow degrees of freedom, one can construct the corresponding relaxed map more appropriate for the discussion of the dynamics and stability, as was shown in Sec. III.

V. CONCLUSION

We analyze a simple model of dispersive bistability in a ring cavity filled with a slow nonlinear medium in the presence of two and three different frequencies. The steady-state characteristics are shown and the condition
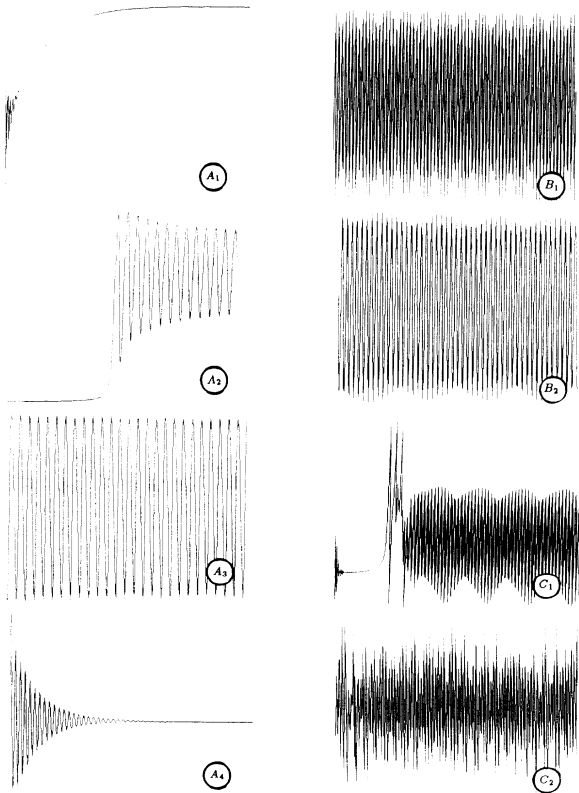
for a selective switching is studied. The characteristic phenomenon of locking of the output intensities is presented. The effect of the finite response time of the nonlinear medium on the stability of the steady states and on the dynamics is discussed in the framework of generalized Ikeda maps. Phenomenological description of the dynamics incorporated into a round-trip map allows one to relate directly the condition for numerical stability of the algorithm with those for physical stability.

ACKNOWLEDGMENT

[1] H. M. Gibbs, *Optical Bistability: Controlling Light with Light* (Academic, New York, 1985).

[2] L. Lugiato, Prog. Opt. XXI, 71 (1984).

[3] J. C. Englund, R. P. Snapp, and W. C. Schieve, Prog. Opt. XXI, 357 (1984).

[4] S. W. Koch, *Dynamics of First-Order Phase Transition in Equilibrium and Nonequilibrium Systems* (Springer-Verlag, Berlin, 1984).

[5] N. Tsukada and T. Nakayama, Phys. Rev. A **25**, 964 (1982).

[6] D. Kagan, H. Friedman, and A. D. Wilson-Gordon, Opt. Commun. **77**, 53 (1990).

[7] A. Korpel and A. W. Lohmann, Appl. Opt. **25**, 2253 (1986).

[8] F. Marquis, P. Dobiasch, P. Meystre, and E. M. Wright, J. Opt. Soc. Am. B **3**, 50 (1986).

[9] K. Inoue, Opt. Lett. **12**, 918 (1987).

[10] G. P. Agrawal, *Nonlinear Fiber Optics* (Academic, New York, 1989).

[11] J. V. Moloney, F. A. Hopf, and H. M. Gibbs, Phys. Rev. A **25**, 3432 (1982).

[12] D. W. McLaughlin, J. V. Moloney, and A. C. Newell, Phys. Rev. Lett. **54**, 681 (1985).

[13] J. V. Moloney, Phys. Rev. Lett. **53**, 556 (1984).

[14] A. Korpel and P. P. Banerjee, Proc. IEEE **72**, 1109 (1984).

[15] M. Maghraoui and P. P. Banerjee, Opt. Commun. **83**, 358 (1991).

[16] F. Verheest, J. Phys. A **20**, 103 (1982).

[17] C. M. Savage, H. J. Carmichael, and D. F. Walls, Opt. Commun. **42**, 211 (1982).

[18] H. J. Carmichael, C. M. Savage, and D. F. Walls, Phys. Rev. Lett. **50**, 163 (1983).

[19] H. Kawaguchi, H. Tani, and K. Inoue, Opt. Lett. **12**, 513 (1987).

[20] J. H. Marburger and F. S. Felber, Phys. Rev. A **17**, 335 (1978).

[21] W. J. Firth, Opt. Commun. **39**, 343 (1981).

[22] K. Ikeda, Opt. Commun. **30**, 257 (1979).

[23] N. B. Abraham, P. Mandel, and L. M. Narducci, Prog. Opt. XXV, 1 (1988) (see pp. 62 and 63).

[24] P. Pliszka, M. Kolwas, and K. Kolwas, J. Opt. Soc. Am. B **6**, 2363 (1989).

[25] R. May, *Stability and Complexity in Model Ecosystems* (Princeton University, Princeton, NJ, 1974), pp. 26–30 and 200–203.
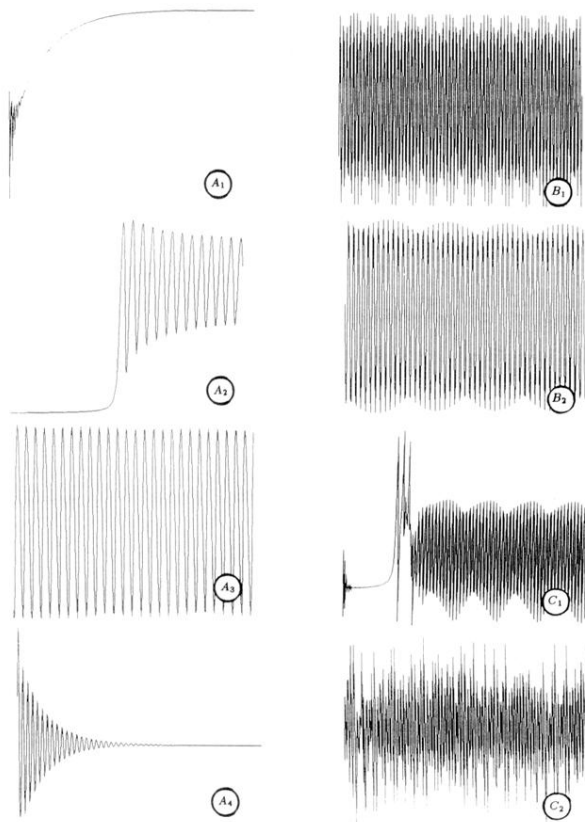
FIG. 7. The I_{out} vs time dependence shown for times up to $300\tau_r$. Plots A and B correspond to different values of α and I_{in} as shown in Fig. 6. Plot C_1: $a=2$, $\alpha=0.03$, $I_{in}=15$, $\Delta\theta=0$. Plot C_2: $a=1$, $\alpha=0.05$, $I_{in}=15$, $\Delta\theta\sim T$.